ELSEVIER

Journal of Organometallic Chemistry 554 (1998) 49–61

Journal of Organometallic Chemistry

Time resolved infrared spectroscopy as a technique to study reactive organometallic intermediates

Karen McFarlane, Brian Lee, Jon Bridgewater, Peter C. Ford *

Department of Chemistry, University of California, Santa Barbara, CA 93106, USA

Received 9 January 1997; received in revised form 15 April 1997

Abstract

The application of time resolved infrared spectroscopy to problems in organometallic chemistry is discussed and an overview of different techniques to record TRIR spectra ranging from μs to fs time scales is presented. More detailed examples of TRIR applications in organometallic chemistry from the authors' laboratory are summarized. These are concerned with elucidating the natures and reaction dynamics of intermediates in the migratory insertion of CO into the metal–alkyl bonds of manganese and cobalt carbonyls and of cyclopentadienyl iron complexes. © 1998 Elsevier Science S.A.

Keywords: Time resolved infrared spectroscopy; Manganese; Cobalt; Iron

1. Introduction

This article will present a brief overview of time resolved infrared spectroscopy (TRIR) applied to the investigation of reactive organometallic intermediates generated photochemically in solution. As discussed here, TRIR is a flash photolysis pump–probe technique where the transients are generated by a laser pulse and the resulting solutions are probed by some type of IR source using very fast infrared detection methodology. This provides the investigator an opportunity to prepare and to interrogate short-lived species relevant to the elucidation of photochemical pathways. Furthermore, appropriate choice of precursors leads to transients which have the same composition as reactive intermediates proposed for stoichiometric models or cyclic reactions of organometallic catalysts. Such intermediates are elusive under thermal conditions owing to the low steady state concentrations which impede direct observation. In this context, preparing non-steady state concentrations of reactive intermediates via flash photolysis and characterizing these by TRIR has proved to be an important strategy in elucidating mechanisms of C–H and H–H bond activation, ligand substitution reactions, migratory insertion and other processes relevant to catalytic and photocatalytic activation of small molecules such as methane and carbon monoxide [1–3]. In this overview, different approaches to obtaining TRIR spectral information will be summarized; however, illustrations of the technique will be largely drawn from ongoing studies in this laboratory relevant to the reactive intermediates in the migratory insertion of CO into metal alkyl bonds.

1.1. Why TRIR?

Elucidating the photochemical mechanism requires identifying each key stage of the excitation and reaction profile. Time resolved techniques allow one to plot the temporal course of events, i.e., the rise and fall of key species such as the excited states (ES), the reactive intermediates generated as the primary photoproducts, and the final products. Infrared detection is particularly useful for spectroscopic characterization and kinetic studies of organometallic reactions since the relevant compounds often include functional groups with characteristic frequencies which are sensitive to molecular structure and conformation as well as the medium. The broad, often featureless, UV/Vis

* Corresponding author.

absorption bands commonly seen for solution phase organometallic compounds by time resolved optical (TRO) spectroscopy generally allow little structural interpretation, and the bands of various species often overlap. The much narrower IR bands give better resolution and often allow for direct observation of the temporal decay and appearance of individual species with minimal interference. However, it should be emphasized that TRIR and TRO are complementary, not competitive, techniques and both should be used when possible. The ensemble of spectroscopic and kinetic information from TRO and TRIR techniques combined with theory and chemical intuition enable elucidation of structures and dynamics of key excited states and reactive intermediates.

Besides excited states, what short-lived species might one expect to detect and identify as well as to follow their temporal course of formation and decay? For a transition metal complex ML_n, the most common photoreaction would be ligand dissociation (Eq. 1). With molecular ligands such as CO or an alkene, dissociation is heterolytic, and the resulting ML_{n-1} intermediate might be expected to have a solvent molecule in the vacant site. On the other hand, metal alkyls and similar species commonly undergo homolytic dissociation to give (17 e^-) radicals. In solution, other relaxation processes are sufficiently fast that one normally expects but a single ligand to be labilized. However, in the gas phase, when there is sufficient excitation energy, multiple dissociations often occur. For polynuclear complexes, metal–metal bonds are often the weakest, and homolytic cleavage to metal radicals competes with ligand dissociation (Eq. 2).

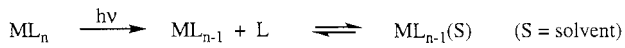

(1)

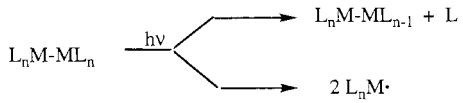

(2)

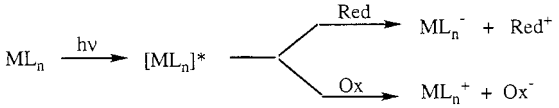

(3)

Such unimolecular processes may occur from very short-lived or even dissociative states. For bimolecular reactions such as electron transfers (Eq. 3), to be competitive, the ES lifetimes must be sufficiently long to participate in diffusive processes.

2. Experimental procedures: TRIR apparatus and techniques

When considering instrumentation for TRIR studies, the key issues are instrumental sensitivity, spectral range and temporal response. The term ‘time resolved infrared spectroscopy’ could apply to any IR frequency vs. time observation of an evolving system. However, we will focus on short-lived systems where solutions cannot be prepared by mixing techniques, but require laser flash photolysis to generate the transients of interest in fluid solutions. A complimentary technique is the photolysis of low temperature frozen solutions or solid matrices. This extends the lifetime of transient species so that spectra may be recorded by conventional spectrometers [4–6]. Similar advantages may be gained by using a low temperature solution such as a liquefied noble gas [7].

Three types of TRIR systems will be summarized here. The first is the conventional laser pump–probe system with a ns pump source and a continuous IR probe source operating at a single (but tunable) IR frequency monitored by a fast rise-time diode detector. The advantage of this system is relative ease of use. The second utilizes step scan FTIR detection techniques which allow much easier data collection over wide frequency ranges. The third involves an ultrafast laser pump source with an IR probe pulse generated in conjunction with the excitation pulse. In that case, temporal responses are determined by differences between the pump and the probe light beam path lengths.

2.1. Conventional ns TRIR systems

In the systems described here, the ns pump source is either a XeCl excimer laser or a Nd:YAG laser with excitation wavelengths determined by harmonic generation or dye lasers. For many metal carbonyl/organometallic complexes, the 308 nm output of the XeCl excimer and the 355 nm third harmonic of the Nd:YAG are convenient, since extinction coefficients at these optical wavelengths are comparable to the extinction coefficients of carbonyl stretching bands in the IR spectrum. The relative stability of these pump sources allows ample signal averaging. For most organometallic systems, the repetitive excitation implied by signal averaging also requires methodology for flowing

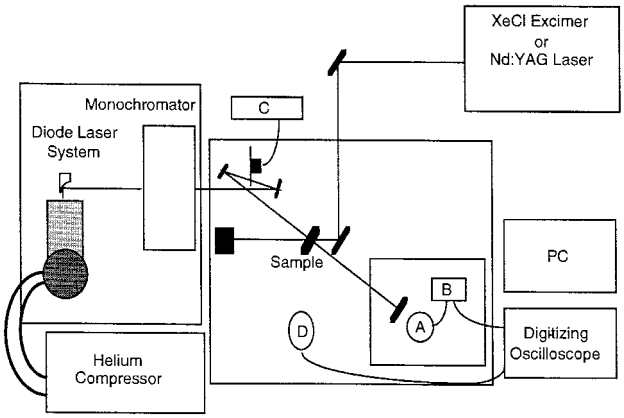

Fig. 1. Schematic diagram of a ns TRIR spectrometer using a lead salt IR diode laser as the probe source. The probe source (Laser Photonics) is based on 3 components: a cold head containing 4 diode lasers cooled by a closed cycle He refrigerator, a collimating assembly which includes a HeNe laser for alignment, and a monochromator to filter unwanted frequencies since at a given i and T, the diode lasers may laser at several modes separated by 1–3 cm^{-1}. The IR beam is directed through a chopper (C), then the sample cell to a HgCdTe (PV) detector (A), the signal from which is amplified by a preamplifier (B) and recorded by a digital oscilloscope. (The chopper is used to obtain $\mathbf{I}_o$, then is removed.) The excitation source is either a XeCl excimer laser or a Nd:YAG laser, either of which can be operated with a dye laser. The sample cell is modified from a commercially available demountable infrared cell with CaF_2 windows. The inlets and outlets of this cell are silver soldered to stainless steel cannula connected to a pump driven flow system designed for constant flow of derated solutions under inert or reactive gas atmospheres.

the sample through the IR and UV/Vis-transmitting sample cell. (The sample cell, flow system and any sample handling hardware must be appropriate for handling air sensitive compounds under various gas mixtures.) The probe is a continuous IR source operating at a single frequency and the IR detector is a fast rise-time photo diode. The system long used in the authors' laboratory [8–13] is illustrated in Fig. 1. This is capable of probing the TRIR of organometallic systems over the ns to the ms time regime.

Three different types of IR probe sources have been used in such systems. In terms of convenient selection of probe frequency, a globar (black body source) combined with a monochromator has proved quite useful in various laboratories [14] but has the problem that the photon flux at any frequency is relatively low (which inherently leads to poor S/N or resolution problems). This problem has been circumvented by the use of CO lasers for TRIR investigations of the photoreactions of metal carbonyls [15]. CO lasers give high monochromatic photon flux (50–500 mW) in an appropriate, but limited, spectral range (2000–1500 cm^{-1}) for investigating metal carbonyls. A CO laser is line tunable but the spacing of the laser frequencies is 4 cm^{-1}. Resolution is improved by also using ^{13}CO in the laser, since the resulting lines fall between those observed when the laser is filled with ^{12}CO.

An IR probe source between black body radiation and CO lasers in single frequency photon flux (0.1–10 mW) is the semiconductor diode IR laser. This is advantageous for its continuous tunability with very high resolution ($< 10^{-3}$ cm^{-1}) [16]. The diodes are manufactured from single crystal 'lead salt' semiconductor alloys. The band gap can be altered by varying the composition, and such diode lasers are available for a broad IR frequency range (370–3050 cm^{-1}). An individual laser of this type generally has a maximum scanning range of < 200 cm^{-1} and is tuned over this region by changing the temperature and current through the diode. The diode operating temperature is low (< 60 K), and early systems required a closed cycle He refrigerator, a major source of noise. Diode IR laser systems that are operated more conveniently at LN_2 temperatures (80–120 K) are now available, although these typically have less output power. The system has up to four lasers in the cold head, so if these have complementary tuning ranges, a total spectral band width for the system up to ~ 700 cm^{-1} might be achieved. (This is somewhat optimistic, since obtaining diode lasers with the exact ranges desired without leaving gaps in the desired spectral range is difficult.) Nonetheless, the frequency ranges available, the high resolution, and the continuously tunable nature of the semiconductor diode IR lasers make this type of source a convenient probe for ns TRIR studies of organometallics in condensed phase.

Signal detection in the ns TRIR systems described in this section is typically achieved with LN_2 cooled HgCdTe and InSb diode IR detectors which can be manufactured with rise-times near 10 ns. HgCdTe is often the material of choice owing to its broad range of spectral response (5000–400 cm^{-1}). Photovoltaic (PV) detectors are generally better for fast response and low noise than the comparable photoconductive (PC) diodes [17]. For the system described in Fig. 1, a fast rise-time preamplifier is used to boost the detector signal, which is recorded on a digital oscilloscope before transferring to a desk top computer for data workup by customized software.

2.2. Flash photolysis with step-scan FTIR detection

The ns techniques using single frequency detection are inconvenient for acquiring data over a broad IR spectral range. Although frequencies of the commercially available IR diode lasers cover most of the range typically used for compound characterization, the TRIR spectrum is generated by laminating together temporal absorbance data obtained one frequency per experiment. Thus, it is a labor intensive process to produce a time-resolved IR spectrum with resolution of 2 cm^{-1} even if the frequency range of interest to characterize a specific system is relatively narrow. In this context, it would be attractive to take advantage of the broad band of frequencies available from a black body IR source in order to record a broader spectrum for short-lived transient species. This can be achieved by using a step-scan interferometer electronically coupled to the repetitive pulse laser.

In FTIR, an interferrogram is generated by recording the intensity of the signal from a black body source passed through a sample and an interferometer as a function of the displacement of a moving mirror. This information is converted to an intensity vs. frequency spectrum by taking the Fourier transform. Alternatively, the interferogram can be generated point-by-point if the mirror were precisely 'stepped' from one fixed position to another and the intensity measured accurately as a function of that mirror position. If the sample is subjected to laser flash photolysis precisely coupled to the detection electronics, then one can record the time dependent intensity at each step of the mirror scan. A Fourier transform of the intensities recorded at a specific time delay for the entire collection data set of mirror step positions gives the IR spectrum for that time, and an ensemble of these spectra as a function of time provides the three dimensional surface of frequency vs. time vs. absorbance. The spectral resolution is determined by the number of interferometer steps and the temporal resolution is determined by the rise-time and sensitivity of the detector and electronics. Step-scan FTIR spectrometers are commercially available but require significant modification for applications in flash photolysis TRIR studies [18–20].

A demonstration of the application of the step-scan FTIR technique in organometallic photochemistry is the recent characterization of the long-lived electronic excited states of the rhenium(I) carbonyl complexes **D** and **E** by Schoonover et al. [18]. The TRIR spectra of **D** and **E**

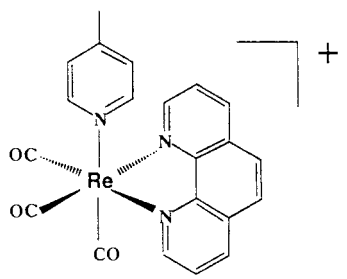

D

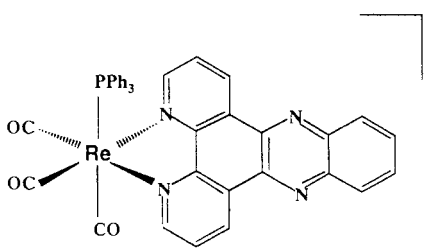

E

acquired 600 ns after excitation clearly show two different patterns. The ground state IR spectrum for **D** displays a ν_{CO} band at 1930 cm^{-1} which splits and shifts to 1962 and 2009 cm^{-1} after 355 nm laser excitation. Such a shift to higher frequency is consistent with formation of a metal-to-ligand-charge-transfer (MLCT) excited state, which one can represent formally as involving the oxidation of Re(I) to Re(II). The higher effective positive charge on the metal leads to diminished backbonding to the π^* orbitals of the CO thus increased ν_{CO}. In contrast, the step scan FTIR difference spectrum recorded upon excitation of **E** under the same conditions displayed three ν_{CO} bands shifted only slightly to lower energy from their corresponding ground state bands. These small shifts are consistent with a ligand-localized $\pi\pi^*$ excited state which would have little impact on the rhenium-CO electronic interactions.

For kinetics studies where temporal absorbance measurements at a selected number of band maxima are desired, the single frequency detection systems described above are especially well suited. However, step-scan FTIR detection has major advantages when time resolved spectral changes over a full frequency range will provide better insight and as a methodology ideal for computer controlled automation. The usefulness of such data is still limited by the intensities of the bands affected by the flash photolysis experiment, but the advantages of full spectral accumulation are likely to be realized as more sensitive detectors become available.

2.3. Ultrafast TRIR systems

A primary difference between ultrafast (ps–fs) and ns time resolved spectroscopy lies in the generation and temporal detection of the probe pulse. Various methods for the TRIR interrogation of short lived transients have recently been the subject of several reviews [21,22], so discussion here will be limited to a general overview of representative ultrafast IR systems.

In ultrafast TRO studies the initial pulse is split into pump and probe pulses. Focusing the probe pulse into a suitable material generates a continuum (i.e., broad band polychromic) pulse by nonlinear processes [23]. This is often split into two beams which are respectively passed through reference and sample then dispersed via spectrograph across a CCD or other optical multichannel type detector. Timing of the experiment is accomplished by spatially delaying the probe pulse from the pump pulse (e.g., 1 ps = 0.3 mm). Signals as small as $\Delta A = 0.001$ are routinely detected. Ultrafast TRIR systems rely on a similar setup to obtain transient spectra, the principal difference being the generation of an IR probe pulse which is typically achieved by nonlinear mixing of visible pulses. Pulse broadening caused by group velocity dispersion may be a problem but is minimized by using very short pathlength mixing crystals. At extremely short pulsewidths, uncertainty broadening also becomes a significant concern, e.g., a 100 fs pulse would have a bandwidth of $\sim 150\ cm^{-1}$. Spectral resolution lost to uncertainty broadening can be recovered by passing the signal through a monochromator after the sample cell [24].

Fig. 2 illustrates an ultrafast TRIR system described by Heilweil and coworkers which utilizes this technique [25]. In this apparatus the broadband IR pulse is generated by frequency mixing in $LiIO_3$ of the second harmonic of a Nd:YAG laser (532 nm) or a Nd:YAG pumped DCM dye laser with the broadband output of a synchronously pumped dye laser also in the visible range. This pulse is split into a reference and a signal pulse, the latter being sent through the sample cell at some temporal delay after the pump pulse. The two IR pulses (ν_{ir}) are each up converted by mixing with 532 nm light (ν_{vis}) in another $LiIO_3$ crystal to give visible light of higher frequency ($\nu = \nu_{ir} + \nu_{vis}$) which allows one to exploit highly sensitive optical detectors. The resulting two visible pulses are dispersed across a CCD detector so that a difference spectrum can be obtained. With this setup, transient spectra of 100 cm^{-1} bandwidth with 4 cm^{-1} spectral resolution, 10^{-3} ΔOD sensitivity and an effective time resolution of 0.4 ps are obtained. Since the dye laser is tunable, the frequency of the resulting IR pulse can also be tuned and the frequencies available should only be limited by the tuning range of the $LiIO_3$ crystal (1800–4000 cm^{-1}).

Hochstrasser and coworkers also use up conversion for TRIR detection of transients on the femtosecond timescale [22,26,27]. In their system the sample is probed by a tunable diode IR laser or a line tunable CO laser at a single frequency which is continuous over the timescale of the experiment. A temporal change in the IR absorbance results from excitation by a fs visible pump pulse, and the time dependent IR absorbance is obtained by up converting a temporal slice of the CW IR beam with a fs visible gate pulse that has been delayed from the pump beam. This up converted pulse ($\nu = \nu_{ir} + \nu_{vis}$) is then detected with a photomultiplier tube. Since CW IR lasers have very narrow linewidths, transient spectra can be obtained with high spectral resolution on a sub-ps timescale without complications of uncertainty broadening.

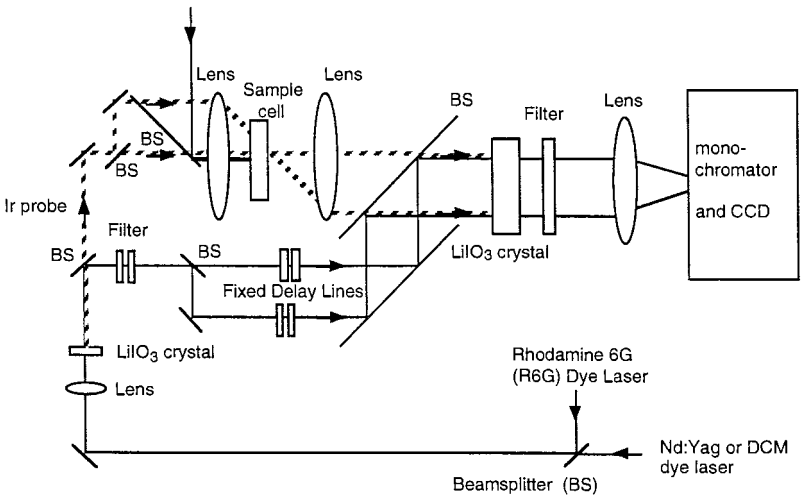

Fig. 2. Schematic of a dual-beam ps TRIR instrument using a broad band IR probe pulse (dashed line) generated by frequency mixing with detection by a CCD camera following up conversion to visible wavelengths. (Adapted from Ref. [25]).

Another detection method used in ultrafast TRIR is to detect the sample and reference IR pulses individually using HgCdTe or InSb detectors. This approach has been successfully employed by Stoutland et al. [21] and Doorn et al. [28] to measure absorbance changes on the order of 10^{-3} with $S/N > 10$ and temporal resolution of ~ 0.5 ps.

An example of the application of ultrafast lasers to an organometallic problem can be drawn from photochemical studies of the $[CpFe(CO)_2]_2$ dimer ($Cp = \eta^5\text{-}C_5H_5$), which has been shown to display two reactive pathways [29,30]. Visible photolysis results primarily in Fe–Fe bond homolysis to give radicals; UV photolysis leads to intermediates from decarbonylation (Eq. 4). Low temperature experiments with IR detection as well as ambient temperature μs TRIR experiments have shown the decarbonylated dimer $Cp_2Fe_2(CO)_3$ to be the triply-bridged dimer (**T**) [31,32].

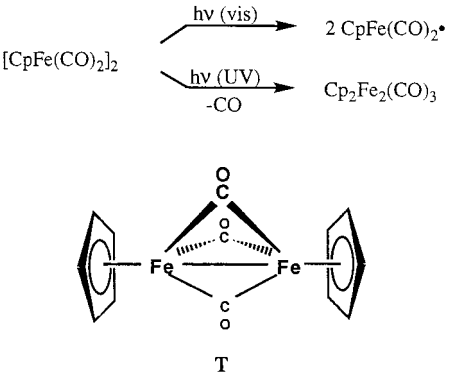

T

(4)

Subsequent ns TRIR studies found **T** to be unreactive toward THF even though $Cp_2Fe_2(CO)_3(THF)$ is also formed when $[CpFe(CO)_2]_2$ was photolyzed in THF [33,34]. To accommodate this observation, a scheme incorporating a very short-lived intermediate species **X** as a common precursor to both **T** and $Cp_2Fe_2(CO)_3(THF)$ was proposed [34]. Ultrafast TRIR investigations using visible [27,35,36] and UV [37] excitation in various solvent media were carried out to address the natures and reactivities of these intermediates. In the former case (visible excitation) homolytic metal–metal bond cleavage dominates and geminate recombination of the radical pairs within the solvent cage could be followed by monitoring dimer reformation on the fs timescale. In the latter case where CO dissociation dominates, a key issue was to identify the precursor(s) to **T** and $Cp_2Fe_2(CO)_3(THF)$.

In this context, George et al. [37] were able to demonstrate that the TRIR spectrum after ps UV photolysis (289 nm) of $[CpFe(CO)_2]_2$ in *n*-hexane leads to formation of **T** with $\nu_{CO} = 1824\ cm^{-1}$ within 10 ps. Sharpening of this IR band, indicative of vibrational cooling, occurred over the course of 140 ps. A band at ν_{CO} 1935 cm^{-1} consistent with that assigned to $CpFe(CO)_2$ [32] was also observed at $\Delta t = 35$ ps as well as a small absorbance at $\sim 1910\ cm^{-1}$ for an unknown intermediate species **Y.** The latter increases in intensity and narrows over the period 35 to 560 ps. In THF, a transient spectrum taken after 240 ps showed no evidence of the 1908 cm^{-1} peak, but instead two absorbance maxima at 1935 cm^{-1} and 1945 cm^{-1} appeared. The weak 1945 cm^{-1} absorbance corresponded to the ν_{CO} characterized by Moore et al. [32] as $Cp_2Fe_2(CO)_3(THF)$. In 10/90 THF/*n*-hexane, the 1908 cm^{-1} band but not the 1945 cm^{-1} band could be observed $\Delta t = 30$ ps (Fig. 3). As $\Delta t = 250$ ps, the absorption at 1908 cm^{-1} decreases with concomitant growth of an absorbance peak at 1945 cm^{-1} with a rate constant estimated as $\sim 1 \times 10^{10}\ s^{-1}$. Since **T** is not formed from **Y**, the suggestion that there is a common intermediate (**X**) to both **T** and to $Cp_2Fe_2(CO)_3(THF)$ does not appear to be substantiated.

$$\underset{1908\,cm^{-1}}{Y} + THF \rightarrow \underset{1945\,cm^{-1}}{Cp_2Fe_2(CO)_3(THF)} \qquad (5)$$

3. TRIR studies of reactive intermediates in CO migratory insertion

The formation of carbon–carbon bonds via a CO 'migratory insertion' mechanism has been studied extensively using the prototypes $Mn(CO)_5R$ and $CpFe(CO)_2R$ ($Cp = \eta^5 - C_5H_5$) [38–41]. The interest in this fundamental reaction draws in large part from its roles in various catalytic schemes such as methanol carbonylation to acetic acid and alkene hydroformylation [42]. Kinetic studies of the iron and manganese models support a rapid equilibrium

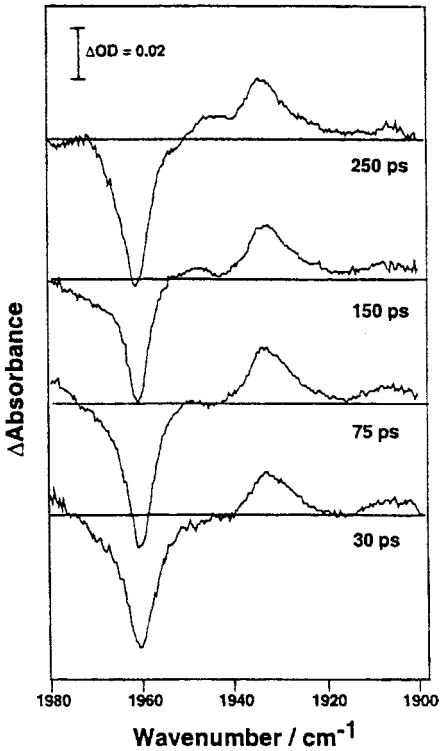

Fig. 3. Transient IR spectra following 289 nm photolysis of $[CpFe(CO)_2]_2$ in *n*-hexane doped with 10% THF at four values of Δt (pump-probe delay time). Figure adapted from Ref. [37].

between the parent complex (**M**) and a thermally generated acyl intermediate ($\mathbf{I}_{th}$) which may then be trapped by a ligand 'L' to form **A** (Eq. (6)).

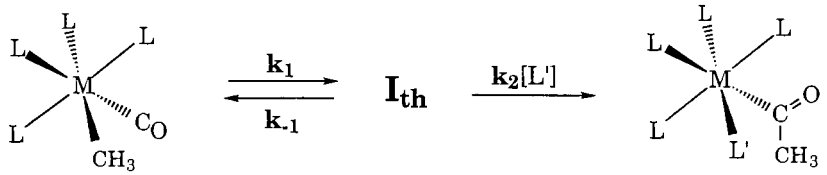

(6)

Despite the attention this reaction mechanism has attracted, the structure and reactivity of $\mathbf{I}_{th}$ have remained elusive [38]. In this context we have been using TRIR to elucidate mechanisms relevant to the carbonylation of metal–alkyl bonds [8–13,43–47]. Summarized here are some ns TRIR studies of the 'unsaturated' intermediates $Mn(CO)_4(COCH_3)$ and $CpFe(CO)(COCH_3)$ and some preliminary results on the catalytic intermediate species $Co(CO)_2(PPh_3)(COCH_3)$.

In order to interrogate intermediates relevant to the thermal carbonylation of alkyl complexes, the strategy used in these laboratories entails forming the intermediates photochemically. Laser flash photolysis of **A** results in photoejection of CO to give non-steady-state concentrations of the coordinatively unsaturated intermediate $\mathbf{I}_p$ (Eq. (7)). From their TRIR spectra in the ν_{CO} region, such species can be detected and identified. Under thermal conditions, steady-state concentrations of such reactive transients would generally be too low to allow IR detection.

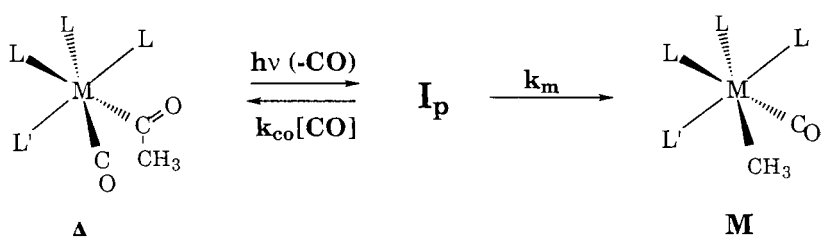

(7)

Probing temporal changes of terminal and acyl ν_{CO} absorbance bands corresponding to the intermediate and products enables determination of infrared spectral characteristics of $\mathbf{I}_p$ and kinetic parameters corresponding to the methyl migration pathway (k_m) and the ligand-substitution pathway (k_L) (Eq. (8)). If $\mathbf{I}_p$ and $\mathbf{I}_{th}$ are equivalent, k_m and k_L are analogous to k_{-1} and k_2, respectively. The lifetimes of the intermediates studied were typically between 10 ms and 1 μs, thus ns TRIR spectroscopy is well suited for the majority of these investigations. In some cases, the lifetimes were too long and time resolved optical (TRO) detection was implemented.

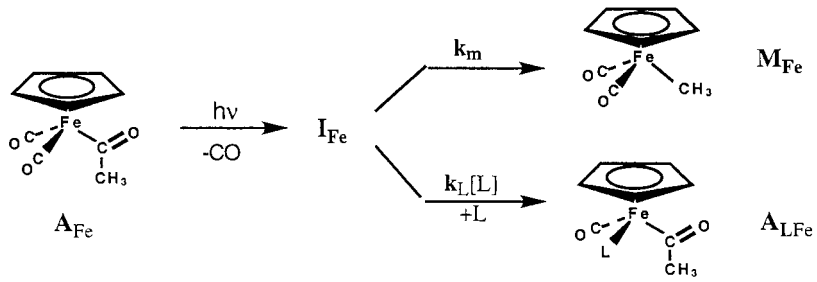

(8)

3.1. Investigations of $CpFe(CO)_2R$ [9,12,13,47]

Continuous wave photolysis (313 nm) of the acetyl complex $CpFe(CO)_2(COCH_3)$ ($\mathbf{A}_{Fe}$) results in clean formation of the methyl complex $CpFe(CO)_2(CH_3)$ ($\mathbf{M}_{Fe}$) with good efficiency ($\Phi = 0.62$ in organic solvents). This quantum yield is not affected by P_{CO} up to 1 atm CO, indicating that the rate constant for the back–reaction of $\mathbf{I}_{Fe}$ with CO is not competitive with methyl migration at $[CO] \leq 0.01$ M. However, in the presence of a ligand (L) such as $P(OMe)_3$ under the conditions $[L] > 0.001$ M, the ligand substituted acetyl product $CpFe(CO)L(COCH_3)$ (A_{LFe}) was also detected spectroscopically.

Laser flash photolysis (308 nm) of $\mathbf{A}_{Fe}$ with TRIR detection in ambient temperature fluid solutions led to the observation of the intermediate $CpFe(CO)(COCH_3)$ ($\mathbf{I}_{Fe}$) (Eq. (8)) within the pulse length of the 20 ns laser flash. A species with a single terminal ν_{CO} absorbance was generated (Fig. 4).

Table 1 lists the IR spectral data for the parent complex ($\mathbf{A}_{Fe}$) and for the intermediate $\mathbf{I}_{Fe}$. In the better donor solvents, the ν_{CO}(terminal) band appears at lower frequencies, indicating that $\mathbf{I}_{Fe}$ is solvated. Kinetic studies were consistent with this assignment; the rates of ligand substitution ($\mathbf{L} = P(OCH_3)_3$) were slower in solvents that are expected to have higher metal–solvent bond energies. An exception to the purported solvento species is in the case of PFMC (perfluoro(methylcyclohexane)) solution. However, in this case, an η^2-acyl or an agostic interaction would give alternative structures likely to be more stable than the solvento species $CpFe(CO)(PFMC)(COCH_3)$.

Table 1 also summarizes data for the spectra of $\mathbf{A}_{Fe}$ and $\mathbf{I}_{Fe}$ recorded in a variable T infrared cell at -78°C. Under these conditions, photochemically generated $\mathbf{I}_{Fe}$ is sufficiently long-lived that its spectrum can be recorded using a FTIR spectrometer. These data suggest that there is little change in the structure of $\mathbf{I}_{Fe}$ between 22 and -78°C in THF (i.e., it is the solvento species at both temperatures). On the other hand there appears to be a change, perhaps to a η^2-acyl complex for $\mathbf{I}_{Fe}$ in -78°C glassy methylcyclohexane.

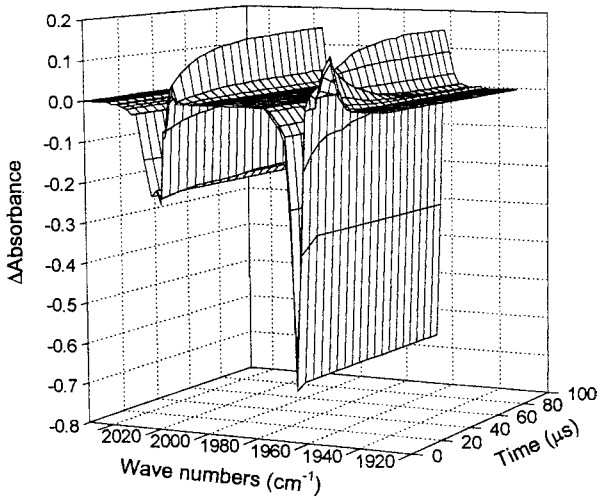

Fig. 4. Temporal Absorbance changes following 308 nm laser flash photolysis of $\mathbf{A}_{Fe}$ (cyclohexane, argon, 23°C).

Table 1
Spectral data for $CpFe(CO)_2(COCH_3)$ ($\mathbf{A}_{Fe}$) and $CpFe(CO)(COCH_3)$ ($\mathbf{I}_{Fe}$) determined by TRIR (22°C) and FTIR (−78°C) spectroscopy; rate constants k_m and k_L ($L = P(OCH_3)_3$) at 22°C under argon atmosphere

Solvent	$\nu_{CO}(A_{Fe})$ (cm^{-1})	$\nu_{CO}(I_{Fe})$[a] (cm^{-1})	k_m (s^{-1})	k_L ($M^{-1}s^{-1}$)	Ref.
PFMC[b]	2025, 1969, 1676	1959	9.4×10^4	1.4×10^7	[12,13]
c-Hexane	2018, 1963, 1669	1949	6.1×10^4	3.6×10^6	[9,12,13]
CH_2Cl_2	2020, 1961, 1620/1598	1940	1.4×10^5	4.3×10^5	[12,13]
DCE[c]	2019, 1959, 1650/1609	1935	1.5×10^5	4.3×10^5	[12,13]
Me_4 THF[d]	2017, 1962, 1669	1921	3×10^5	*e*	[12,13]
2-Me THF	2016, 1955, 1659	1920	3.9×10^4	3×10^5	[12,13]
THF	2015, 1955, 1658	1921	5.6×10^3	2.6×10^4	[9,12,13]
Acetonitrile	2018, 1958, 1650	1926	< 1	$< 10^2$	[9,12,13]
MCH[f,g]	2023/2018, 1968/1962, 1670/1627	1936, 1585	–	–	[12,13]
THF[g]	2013, 1958, 1656	1917, ~1610	–	–	[12,13]

[a]A low signal to noise ratio in the 1600 cm^{-1} region inhibited detection of an intermediate acyl ν_{CO} absorbance bands, thus only $\nu_{CO(terminal)}$ values are reported for room temperature TRIR experiments.
[b]Perfluoro(methylcyclohexane).
[c]1,2-Dichloroethane.
[d]2,2,5,5-Tetramethyl tetrahydrofuran.
[e]Not measured.
[f]Methylcyclohexane.
[g]$T = -78$°C.

Table 1 also lists rate constants corresponding to the ligand substitution (k_L, $\mathbf{L} = P(OMe)_3$) and methyl migration (k_m) reactions of $\mathbf{I}_{Fe}$ obtained from the TRIR data.

In order to investigate the possibility of a ring-slippage mechanism to give an η^3-Cp intermediate along the substitution pathway [47], the system was tested for the 'indenyl effect' [48]. Accordingly, TRIR studies were carried out on the reaction of the photochemically generated indenyl acetyl intermediate $(Ind)Fe(CO)(COCH_3)$ ($Ind = \eta^5$-C_9H_7) with $\mathbf{L} = CO$, PPh_3 and $P(OCH_3)_3$ (Eq. (9)). The intermediate TRIR spectrum displayed a single ν_{CO} band similar to that of $\mathbf{I}_{Fe}$ which decayed to the methyl dicarbonyl within a few μs (Fig. 5). Although the TRIR kinetic studies showed that the indenyl intermediate species underwent unimolecular rearrangement to give the migration product $\mathbf{M}_{Ind}$ with a rate five times that of the Cp compound, there was no spectroscopic evidence for a dicarbonyl

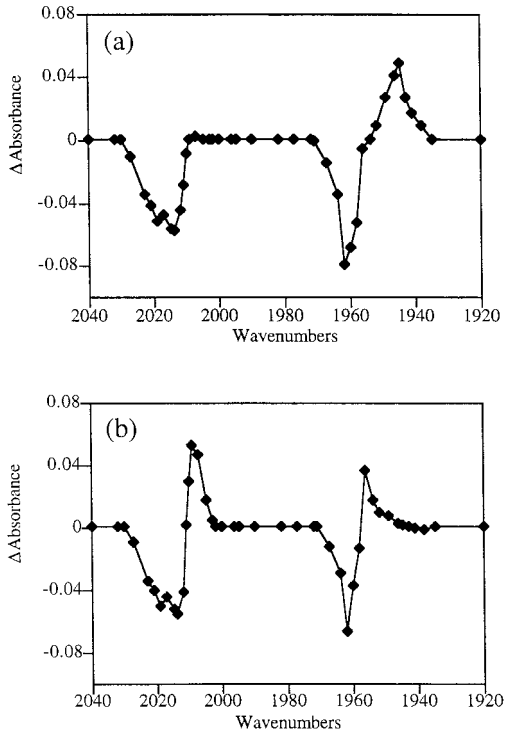

Fig. 5. (a) ΔAbsorbance at 0.2 μs following 308 nm laser flash photolysis of $(Ind)Fe(CO)_2(COCH_3)$. (b) ΔAbsorbance at 14 μs following 308 nm laser flash photolysis of $(Ind)Fe(CO)_2(COCH_3)$. Conditions: cyclohexane, argon, 22°C.

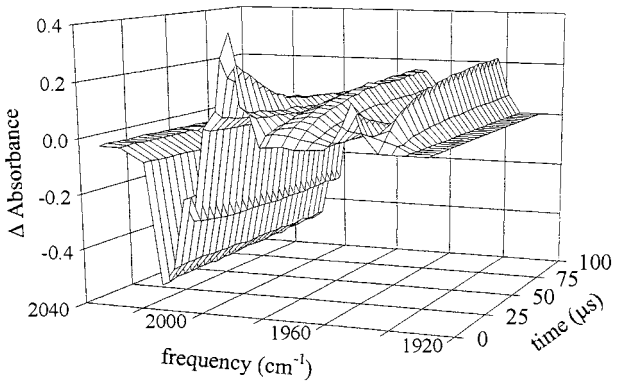

Fig. 6. IR spectral changes following 308 nm photolysis of $\mathbf{A}_{Mn}$ in cyclohexane in the presence of 6.0 mM 4-phenylpyridine. Spectra are spaced at 4 μs intervals. Adapted from Ref. [45].

transient, such as (η^3-Ind)Fe(CO)$_2$(Sol)(COCH$_3$) or (η^3-Ind)Fe(CO)$_2$(L)(COCH$_3$). The k_L was also $\sim 5\times$ faster for the indenyl intermediate consistent with ligand electronic effects far more subtle than would be expected on replacing Cp with Ind if the ring slip mechanism were operating. The absence of an indenyl effect is consistent with studies on the reverse thermal reactions of (Ind)Fe(CO)$_2$(CH$_3$) with various ligands [49–51].

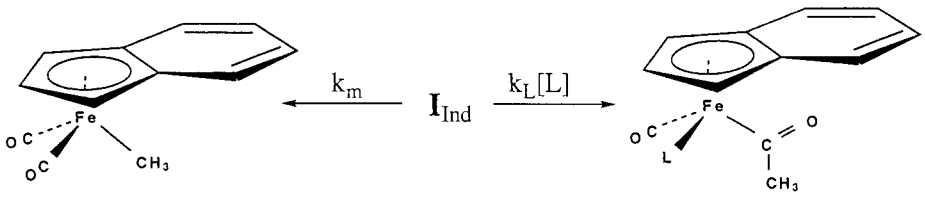

(9)

3.2. TRIR investigations of Mn(CO)$_5$R [43–45]

By the same methodology employed to study the iron system, structural and mechanistic information about the 'unsaturated' intermediate in the carbonylation of Mn(CO)$_5$CH$_3$ ($\mathbf{M}_{Mn}$) was obtained using TRIR (and TRO) spectroscopy. Again, laser flash photolysis led to decarbonylation of the acetyl complex Mn(CO)$_5$(COCH$_3$) ($\mathbf{A}_{Mn}$) to give an intermediate ($\mathbf{I}_{Mn}$) which underwent methyl migration to form $\mathbf{M}_{Mn}$ in competition with recombination with CO to give $\mathbf{A}_{Mn}$, or trapping with a different L to form substituted complexes *cis*-Mn(CO)$_4$(L)(COCH$_3$) ($\mathbf{A}_{LMn}$) (Eq. 10). Fig. 6 shows the transient spectrum of $\mathbf{I}_{Mn}$ and the temporal absorbance changes as it reacts with 4-phenylpyridine to form $\mathbf{A}_{LMn}$ in cyclohexane.

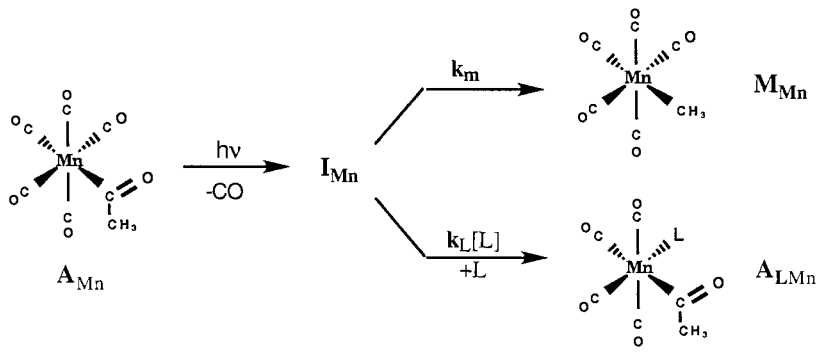

(10)

Continuous wave photolysis (313 nm) of $\mathbf{A}_{Mn}$ at room temperature in various organic solvents results in formation of $\mathbf{M}_{Mn}$ with good photochemical efficiency under argon ($\Phi = 0.62$), and the reaction is inhibited by added CO in accord with this model.

Table 2
Spectral data for $Mn(CO)_4(COCH_3)$ ($\mathbf{I}_{Mn}$) determined by TRIR spectroscopy at 295 K and FTIR spectroscopy at −78°C (data from Ref. [45])

Solvent	ν_{CO} ($\mathbf{I}_{Mn}$) at RT (cm^{-1})	ν_{CO} ($\mathbf{I}_{Mn}$) at −78°C (cm^{-1})
PFMC	1997, 1959	2083 (w) 1998, 1958
c-Hexane	1990, 1952, 1607 (w)	
MCH	1990, 1952	2080 (w), 1988, 1941, 1607 (w)
CH_2Cl_2	1987 (br), 1940 (br)	
Toluene	1984 (br), 1941 (br)	
Me_4THF	1984 (br), 1945 (br)	
2,5-Me_2 THF	1982, 1932(br)	2077 (w), 1979, 1931, 1603 (w)
2-Me THF	1979 (br), 1932 (br)	2077 (w), 1977, 1928, 1600 (w)
THF	1981 (br), 1931 (br)	2077 (w), 1977, 1928, 1602 (w)

The ν_{CO} absorbance bands attributed to $\mathbf{I}_{Mn}$ (Table 2) show a modest sensitivity to solvent. In contrast to the iron system, the transient generated displayed little reactivity over several hundred μs in all solvents investigated. This relatively sluggish reactivity was observed even under CO at $P_{CO} = 1$ atm, although $\mathbf{I}_{Mn}$ eventually decayed to a mixture of $\mathbf{M}_{Mn}$ and $\mathbf{A}_{Mn}$. However, the kinetics of the reaction of $\mathbf{I}_{Mn}$ with CO could be followed using TRO techniques, which had longer time constants.

$\mathbf{I}_{Mn}$ is much less reactive than other 'unsaturated' metal carbonyl intermediates such as $Cr(CO)_5$ which exists as a solvento species in the same weakly coordinating solvents. The acetyl intermediate $\mathbf{I}_{Mn}$ was thus suspected to be stabilized by the acetyl group via an η^2-acyl or an agostic structure. Thus, time resolved spectra and dynamics of the transient species $CH_3Mn(CO)_4(Sol)$ formed by the flash photolysis of $\mathbf{M}_{Mn}$ were examined, since this intermediate should be analogous with the exception that the acetyl functionality is replaced by a simple methyl group. In comparing the reactivities of the two intermediates (see Table 3), it was apparent that there is an enormous difference in their reactivities toward ligands in cyclohexane and perfluoro(methylcyclohexane). In THF the difference is not so dramatic. From these studies it was concluded that the intermediate $\mathbf{I}_{Mn}$ is solvated (**S**) in donor solvents such as THF, while in weakly coordinating solvents such as alkanes, halocarbons and aromatics, the intermediate takes an η^2-acyl structure (**C**).

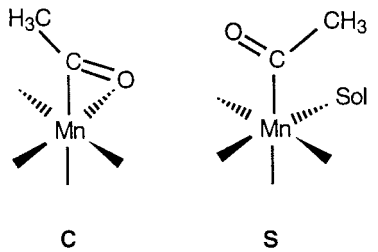

Having established the likely structure of $\mathbf{I}_{Mn}$ in various media, we turn to the effect of solvent on the rate of methyl migration, presumably the microscopic reverse of the first step in the thermal carbonylation reaction. Notably, the trends observed for k_m do not parallel those of the ligand substitution reactions. Although phosphine substitution of $\mathbf{I}_{Mn}$ is three orders of magnitude faster in cyclohexane than in THF, the rate of methyl migration was found to be

Table 3
A comparison of the k_L values for the reactions of $\mathbf{I}_{Mn}$ and $CH_3Mn(CO)_4(Sol)$ with various L in 295 K cyclohexane, PFMC and THF

Solvent	Ligand	k_L for $\mathbf{I}_{Mn}$[a] (M^{-1} s^{-1})	k_L for $CH_3Mn(CO)_4(Sol)$[b] (M^{-1} s^{-1})
Cyclohexane	Phpy	$(7.5 \pm 1.5) \times 10^6$	$(2.5 \pm 0.3) \times 10^9$
Cyclohexane	$P(Ph)_3$	$(2.3 \pm 0.5) \times 10^6$	$(1.0 \pm 0.2) \times 10^9$
Cyclohexane	$P(OMe)_3$	$(1.4 \pm 0.3) \times 10^6$	$(1.1 \pm 0.2) \times 10^9$
THF	$P(OMe)_3$	$(1.7 \pm 0.3) \times 10^3$	
2,2,5,5-Me_4THF	$P(OMe)_3$	6×10^5	
Cyclohexane	CO	$(6.5 \pm 1.3) \times 10^3$	$(4.5 \pm 0.5) \times 10^8$
PFMC	CO	$(1.5 \pm 0.3) \times 10^4$	$(1.0 \pm 0.5) \times 10^{10}$
THF	CO	$< 5 \times 10^2$	$(1.4 \pm 0.3) \times 10^2$

[a] Ref. [45].
[b] Ref. [44].

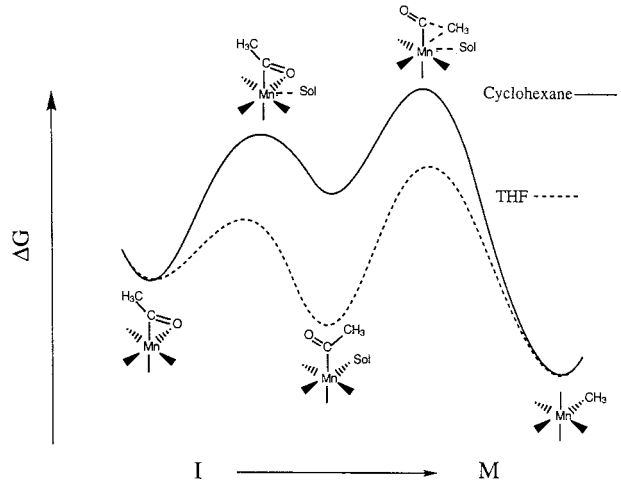

Fig. 7. Free energy profile for k_m pathway from $\mathbf{I}_{Mn}$.

nearly identical in the two solvents. The similar values for k_m in these solvents must be coincidental given the different $\mathbf{I}_{Mn}$ structures in the two solvents. Thus donor solvents tend to favor methyl migration in the competitive reactions of $\mathbf{I}_{Mn}$ because k_L values are depressed.

Fig. 7 illustrates the role of the solvent in promoting methyl migration in a schematic free energy diagram. In weakly coordinating solvents, where $\mathbf{I}_{Mn}$ exists as the η^2-acyl species, the solvent is nonetheless involved in the methyl migration step owing to the solvent dependence of k_m. We propose that the trend of increasing k_m with donating ability of the solvent is the result of the η^2 chelate reacting first to form the solvento species, which then undergoes methyl migration with concerted loss of solvent. This is the microscopic reverse of the previously proposed 'solvent assisted' methyl migration. In THF, the lowest energy form of $\mathbf{I}_{Mn}$ is already the solvento species. Thus, stabilization due to Mn–THF bonding offsets stabilization of the k_m transition state by solvent–metal interactions giving the fortuitous similarity of the $\Delta G_m^{\ddagger}$ values in cyclohexane and THF.

3.3. TRIR investigations of $Co(CO)_3(PPh_3)R$ [46]

Complexes such as $Co(CO)_3(L)R$ (R = hydride, alkyl, acyl) have all been proposed as intermediates derived from $Co_2(CO)_8$/phosphine precursors in the hydroformylation cycle [42]. We have begun studies on these catalytically active species in which the reactive fragments are prepared photochemically and their reactivities interrogated by TRIR. It is intended to determine the reactivities of these intermediates with different ligands (e.g., H_2, CO, olefins) which would be invaluable in the design of catalytic systems.

Continuous wave photolysis of $Co(CO)_3(PPh_3)(COCH_3)$ ($\mathbf{A}_{Co}$) with near-UV radiation in room temperature organic solvents results in formation of $Co(CO)_3(PPh_3)CH_3$ ($\mathbf{M}_{Co}$). Flash photolysis of $\mathbf{A}_{Co}$ in CH_2Cl_2 with TRIR detection leads to observation of an intermediate $\mathbf{I}_{Co}$ with spectral characteristics consistent with CO photoejection, i.e., $Co(CO)_2(PPh_3)(COCH_3)$ (Eq. 11). This intermediate species rearranges to form the methyl complex $\mathbf{M}_{Co}$ with a rate constant of $k_m = 2.0 \times 10^5\ s^{-1}$. In THF, the analogous reaction is faster ($k_m = 1.1 \times 10^6\ s^{-1}$). We plan to adapt our sample handling equipment to accommodate the high gas pressures required to generate various species in the cobalt system.

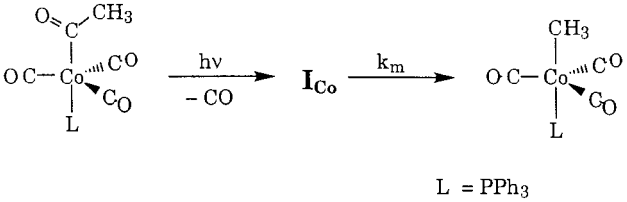

(11)

Acknowledgements

Studies at UCSB have been sponsored by a grant to PCF from the Division of Chemical Sciences, Office of Basic Energy Sciences, U.S. Department of Energy (DE-FG03-85ER13317). Support for instrumentation development came

from a U.S. Department of Energy University Research Instrumentation Grant (No. DE-FG05-91ER79039) and the U.S. National Science Foundation Instrumentation Grant (CHE-9413030). Other individuals contributing to TRIR research at UCSB include J.A. DiBenedetto, D.W. Ryba, S.T. Belt, W.T. Boese and J.G. Rabor.

References

[1] P.C. Ford, W.T. Boese, B.J. Lee, K.L. McFarlane, Photocatalysis Involving Metal Carbonyls, in: M. Graetzel, K. Kalyanasundaram (Eds.), Photosensitization and Photocatalysis by Inorganic and Organometallic Compounds, Kluwer Acad. Publishers, the Netherlands, 1993, pp. 359–390 and refs. therein.
[2] C. Ford, K.L. McFarlane, J. Rabor, W.T. Boese, Coord. Chem. Rev., in press.
[3] M.W. George, M. Poliakoff, J.J. Turner, Analyst 119 (1994) 551–560.
[4] T.E. Bitterwolf, K.A. Lott, A.J. Rest, J. Mascetti, J. Organomet. Chem. 419 (1991) 113–126.
[5] F. W. Grevels, W.E. Klotzbucher, G. Russel, K. Schaffner, Recl. Trav. Chim. Pays-Bas 114 (1995) 571–576.
[6] J.J. Turner, in: Photoprocess in Transition Metal Complexes, Biosystems and Other Molecules, E. Kochanski (Ed.), Kluwer Academic Publishers, the Netherlands, 1992, pp. 113–123.
[7] B.H. Weiller, E.P. Wasserman, C.B. Moore, R.G. Bergman, J. Am. Chem. Soc. 115 (1993) 4326–4330.
[8] J.A. DiBenedetto, D.W. Ryba, P.C. Ford, Inorg. Chem. 27 (1989) 3503–3507.
[9] S.T. Belt, D.W. Ryba, P.C. Ford, J. Am. Chem. Soc. 113 (1991) 9524–9528.
[10] P.C. Ford, J.A. DiBenedetto, D.W. Ryba, S.T. Belt, SPIE Proc. 1636 (1992) 9–16.
[11] C.P. Casey, W.T. Boese, R.S. Carino, P.C. Ford, Organometallics 15 (1996) 2189–2191.
[12] K.L. McFarlane, PhD Dissertation, University of California, Santa Barbara, CA, 1996.
[13] K.L. McFarlane, B. Lee, W. Fu, R. van Eldik, P.C. Ford, Manuscript in preparation.
[14] H. Hermann, F.W. Grevels, H. Henne, K. Schaffner, J. Phys. Chem. 86 (1982) 5151–5154.
[15] M. Poliakoff, E. Weitz, in: Advances in Organometallic Chemistry, Vol. 25, F.G.A. Stone, R. West (Eds.), Academic Press, San Diego, CA, 1986, pp. 277–316.
[16] Laser Photonics, In: Laser Photonics, Analytical division brochure, Laser Photonics, Andover, MA, p. 992.
[17] Santa Barbara Research Center (SBRC) Infrared Components Brochure 17th edn., Santa Barbara Research Center, Goleta, CA.
[18] J.R. Schoonover, G.F. Strouse, R.B. Dyer, W.D. Bates, P. Chen, T.J. Meyer, Inorg. Chem. 35 (1996) 273–274.
[19] C.J. Manning, R.A. Palmer, J.L. Chao, Rev. Sci. Instrum. 62 (1991) 1219–1229.
[20] J.R. Schoonover, G.F. Strouse, K.M. Omberg, R.B. Dyer, Comm. Inorg. Chem. 18 (1996) 165–188.
[21] P.O. Stoutland, R.B. Dyer, W.H. Woodruff, Science 257 (1992) 1913–1917.
[22] K. Wynne, R.M. Hochstrasser, Chem. Phys. 193 (1995) 211–236.
[23] R.R. Alfano (Ed.), The Supercontinuum Laser Source, Springer-Verlag, New York, 1989.
[24] E.J. Heilweil, Opt. Lett. 14 (1989) 551–553.
[25] T.P. Dougherty, E.J. Heilweil, Opt. Lett. 19 (1994) 129–131.
[26] P. Anfinrud, C. Han, P.A. Hansen, J.N. Moore, R.M. Hochstrasser, Picosecond and Femtosecond Infrared Spectroscopy with CW Diode Lasers, in: T. Yajima, K. Yoshihara, C.B. Harris, S. Shionoya (Eds.), Springer Series in Chemical Physics, Vol. 48, Ultrafast Phenomena VI, Springer-Verlag, Berlin, 1988, pp. 442–446.
[27] P.A. Anfinrud, C. Han, T. Lian, R.M. Hochstrasser, J. Phys. Chem. 95 (1991) 574–578.
[28] S.K. Doorn, R.B. Dyer, P.O. Stoutland, W.H. Woodruff, J. Am. Chem. Soc. 115 (1993) 6398–6405.
[29] T.J. Meyer, J.V. Caspar, Chem. Rev. 85 (1985) 187.
[30] J.V. Caspar, T.J. Meyer, J. Am. Chem. Soc. 102 (1980) 7794.
[31] R.H. Hooker, K.A. Mahmoud, A.J. Rest, J. Chem. Soc., Chem. Commun., 1983, 1022.
[32] B.D. Moore, M.B. Simpson, M. Poliakoff, J.J. Turner, J. Chem. Soc., Chem. Commun., 1984, 972.
[33] J.P. Blaha, B.E. Bursten, J.C. Dewan, R.B. Frankel, C.W. Randolf, B.A. Wilson, M.S. Wrighton, J. Am. Chem. Soc. 107 (1985) 4561.
[34] A.J. Dixon, M.W. George, C. Hughes, M. Poliakoff, J.J. Turner, J. Am. Chem. Soc. 114 (1992) 1719.
[35] J.N. Moore, P.A. Hansen, R.M. Hochstrasser, J. Am. Chem. Soc. 111 (1989) 4563.
[36] P.A. Anfinrud, C. Han, T. Lian, R.M. Hochstrasser, J. Phys. Chem. 94 (1990) 1180.
[37] M. George, T.P. Dougherty, E.J. Heilweil, J. Phys. Chem. 100 (1996) 201.
[38] J.P. Collman, L.S. Hegedus, J.R. Norton, R.G. Finke, Principles and Applications of Organotransition Metal Chemistry, Chap. 6, University Science Books, Mill Valley, CA, 1987.
[39] A. Wojcicki, Adv. Organomet. Chem. 11 (1973) 87–145.
[40] F. Calderazzo, Angew. Chem., Int. Ed. Engl. 16 (1977) 299–311.
[41] T.C. Flood, Top. Stereochem. 12 (1981) 37–118.
[42] G.W. Parshall, S.D. Ittle, Homogeneous Catalysis, 2nd edn., Wiley-Interscience, New York, 1992.
[43] W.T. Boese, B.L. Lee, D.W. Ryba, S.T. Belt, P.C. Ford, Organometallics 12 (1993) 4739–4741.
[44] W.T. Boese, P.C. Ford, Organometallics 13 (1994) 3525–3531.
[45] W.T. Boese, P.C. Ford, J. Am. Chem. Soc. 117 (1995) 8381–8391.
[46] J. Rabor, Studies in progress.
[47] D.W. Ryba, R. van Eldik, P.C. Ford, Organometallics 12 (1993) 104–107.
[48] M.E. Rerek, F. Basolo, Organometallics 2 (1983) 372–376.
[49] T.C. Forschner, A.R. Cutler, J. Organomet. Chem., 1989, p. 361.
[50] D. Monti, M. Bassetti, J. Am. Chem. Soc. 115 (1993) 4658–4664.
[51] M. Allevi, M. Bassetti, C. Lo Sterzo, D. Monti, J. Chem. Soc., Dalton Trans., 1996, pp. 3727–3531.